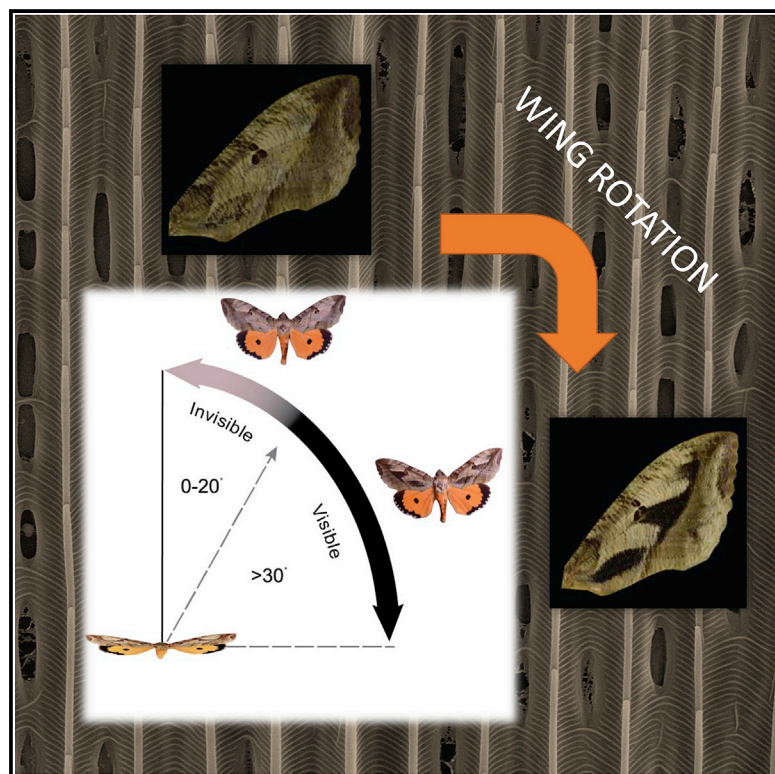


Current Biology

A Dynamic Optical Signal in a Nocturnal Moth

Graphical Abstract



Authors

Jennifer L. Kelley, Nikolai J. Tatarnic, Gerd E. Schröder-Turk, John A. Endler, Bodo D. Wilts

Correspondence

jennifer.kelley@uwa.edu.au (J.L.K.), bodo.wilts@unifr.ch (B.D.W.)

In Brief

Butterflies often produce wing colors that can switch on/off with viewing angle, but Kelley et al. report a nocturnal moth with patterns that change in shape and position with viewing angle. These effects are generated using specialized mirror-like nanostructures, yielding dynamic patterns that may facilitate signaling in dim light.

Highlights

- Novel angle-dependent coloration in nocturnal Lepidoptera
- Wing patches of a night-flying moth change in size, depending on viewing angle
- Nanostructures in the wing scales produce this optical effect
- Dynamic patterns may function for visual signaling in dim light



A Dynamic Optical Signal in a Nocturnal Moth

Jennifer L. Kelley,^{1,8,*} Nikolai J. Tatarnic,^{1,2} Gerd E. Schröder-Turk,^{3,4,5} John A. Endler,⁶ and Bodo D. Wilts^{7,*}

¹School of Biological Sciences, The University of Western Australia, Perth, WA 6009, Australia

²Western Australian Museum, Locked bag 49, Welshpool DC, Perth, WA 6986, Australia

³Mathematics and Statistics, Murdoch University, Perth, WA 6150, Australia

⁴Department of Food Science, Copenhagen University, Rolighedsvej 26, 1958 Frederiksberg C, Denmark

⁵Physical Chemistry, Lund University, Naturvetarvägen 14, 221 00 Lund, Sweden

⁶School of Life & Environmental Sciences, Deakin University, Waurn Ponds, 3216 VIC, Australia

⁷Adolphe Merkle Institute, University of Fribourg, Chemin des Verdiers 4, Fribourg 1700, Switzerland

⁸Lead Contact

*Correspondence: jennifer.kelley@uwa.edu.au (J.L.K.), bodo.wilts@unifr.ch (B.D.W.)

<https://doi.org/10.1016/j.cub.2019.07.005>

SUMMARY

The wings of butterflies and moths generate some of the most spectacular visual displays observed in nature [1–3]. Particularly striking effects are seen when light interferes with nanostructure materials in the wing scales, generating bright, directional colors that often serve as dynamic visual signals [4]. Structural coloration is not known in night-flying Lepidoptera, yet here we show a highly unusual form of wing coloration in a nocturnal, sexually dimorphic moth, *Eudocima materna* (Noctuidae). Males feature three dark wing patches on the dorsal forewings, and the apparent size of these patches strongly varies depending on the angle of the wing to the viewer. These optical special effects are generated using specialized wing scales that are tilted on the wing and behave like mirrors. At near-normal incidence of light, these “mirror scales” act as thin-film reflectors to produce a sparkly effect, but when light is incident at $\sim 20^\circ$ – 30° from normal, the reflectance spectrum is dominated by the diffuse scattering of the underlying, black melanin-containing scales, causing a shape-shifting effect. The strong sexual dimorphism in the arrangement and architecture of the scale nanostructures suggests that these patterns might function for sexual signaling. Flickering of the male’s wings would yield a flashing, supernormal visual stimulus [5] to a viewer located 20° – 30° away from the vertical, while being invisible to a viewer directly above the animal. Our findings reveal a novel use of structural coloration in nature that yields a dynamic, time-dependent achromatic optical signal that may be optimized for visual signaling in dim light.

RESULTS AND DISCUSSION

The Dot-underwing moth, *Eudocima materna* (Linnaeus, 1767), is a large (~ 90 mm wing span) fruit-piercing moth with an extensive range that includes Africa, the South Palaearctic, the Indo-Australian regions and the Central Pacific. The adult moths are

nocturnal feeders, showing peak foraging activities just before midnight and are well known for causing extensive damage to fruit crops [6]. The species is strongly sexually dimorphic; males feature three dark patches on the brown dorsal forewing that change in size depending on the angle of the wing relative to the viewer (Figure 1A; see also Video S1), while in females, the whole surface of the dorsal forewing gradually darkens with changing angle (Figures 1B, S2A, and S2B). In males, the total size of the dark patches increases with horizontal rotation about the long body axis (roll), reaching a maximum size at an angle of approximately 20° – 30° away from normal (Figure 1A). Each of the males’ three wing patches appears or disappears in succession. With rotation toward the viewer, the wing patch closest to the body appears first (patch 1, 10° – 20°), with the outer patches appearing later (patches 2 and 3, 20° – 30°) (Figure 1A). For wing movement away from the viewer, the reverse is true and the outermost patches appear first (Figure 1A; patch 2 and 3, 10° – 20° ; patch 1, 20° – 30° ; see Figure S1 for data for males 2 and 3). For wing rotation around an axis perpendicular to the long body axis (but in the same plane as the body axis; pitch; Figure S1), the change in patch size observed in males was limited, suggesting these directional effects are linked to the orientation of the scales on the wing surface. In females, changes in patch size and mean patch reflectance (averaged over patch area) with angle were minimal for both roll (Figures 1B and S2A–S2D) and pitch (Figures S2E and S2F) highlighting the strong sexual dimorphism of the effect.

These angle-dependent effects were dependent on the location of the patterning on the wings and differed between the sexes. In males, the directional patterning was limited to the three dark patches on the dorsal forewings, whereas in females, angle-dependent effects occurred across the whole dorsal forewing surface, but the effect was more subtle than in males (Figure 1). To investigate the origin of this angle-dependent patterning in relation to the scale structures, we measured the spatial distribution of scattered light both at the scale lattice (the overlapping arrangement of wing scales) and for isolated scales from different wing regions using *k*-space imaging [7]. The pigmented scale lattice (Figure 2A) and the scatterogram of a single pigmented scale (Figure 2C) from the male’s dorsal hindwing show a diffuse and multidirectional pattern of reflectance (illustrated in Figure 2E), typical for diffusely scattering structures. In contrast, the spatial reflectance of scales from the shape-shifting brown patches of the male dorsal forewings



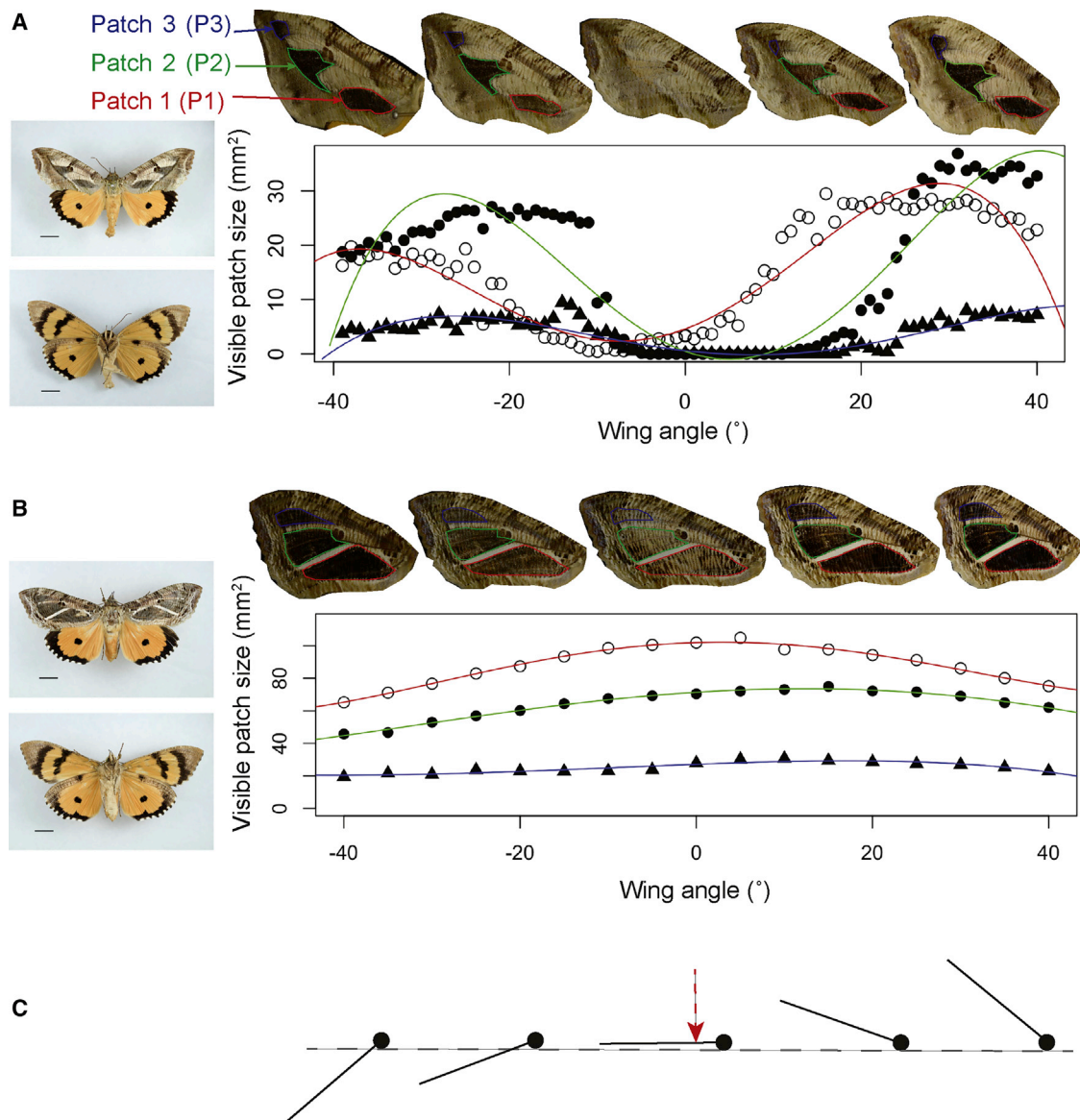


Figure 1. Angle-Dependent Changes in Patterning on the Dorsal Forewings of a Nocturnal Moth, *E. materna*

(A) Successive appearance of three dark patches (red, patch 1; green, patch 2; blue, patch 3) with rotation about the horizontal plane (roll) for male *Eudocima materna* (see also Figure S1 and Video S1).

(B) In females, little change in patch size with angle is observed but the patch darkens overall (see also Figure S2). Dorsal (top) and ventral (bottom) images of males (A) and females (B) are shown in the inset panels (photos by Nikolai Tatarnic; scale bar, 1 cm).

(C) A 0° incidence angle corresponds to incident light being normal to the wing surface (red arrow). Positive values are for movement toward the viewer, negative values for rotation away from the viewer.

shows that light scattering is confined to a narrow band in a direction perpendicular to the scale ridges (Figures 2B, 2D, and 2F). We further determined the optical properties of the different scale types using microspectrophotometry to measure the reflectance and absorbance properties of individual wing scales. The black scales on the hindwings act as broadband absorbers, showing a pattern of reflectance and absorbance that is typical of melanin-based pigments (Figure S3). The orange scales on the hindwings have spectral characteristics comparable to omochrome pigments [8, 9], while the brown and white scales on the forewings absorb in the blue/green and UV parts of the

spectrum, but the exact pigment family is yet to be characterized (Figure S3).

To understand the directionality of the forewing patterning and whether it originates in the scales' nanostructure, we used scanning electron microscopy (SEM; Figure 3). The pigmented scales are similar to the classic Lepidopteran wing scale *bauplan* and feature a thin lower lamina overlaid by a series of open windows formed by parallel ridges and cross ribs (Figures 3A and 3B). This scale structure allows a large fraction of the incident light to reach the lower lamina and be reflected back up to the structured upper lamina to interact with the pigment that is present in both

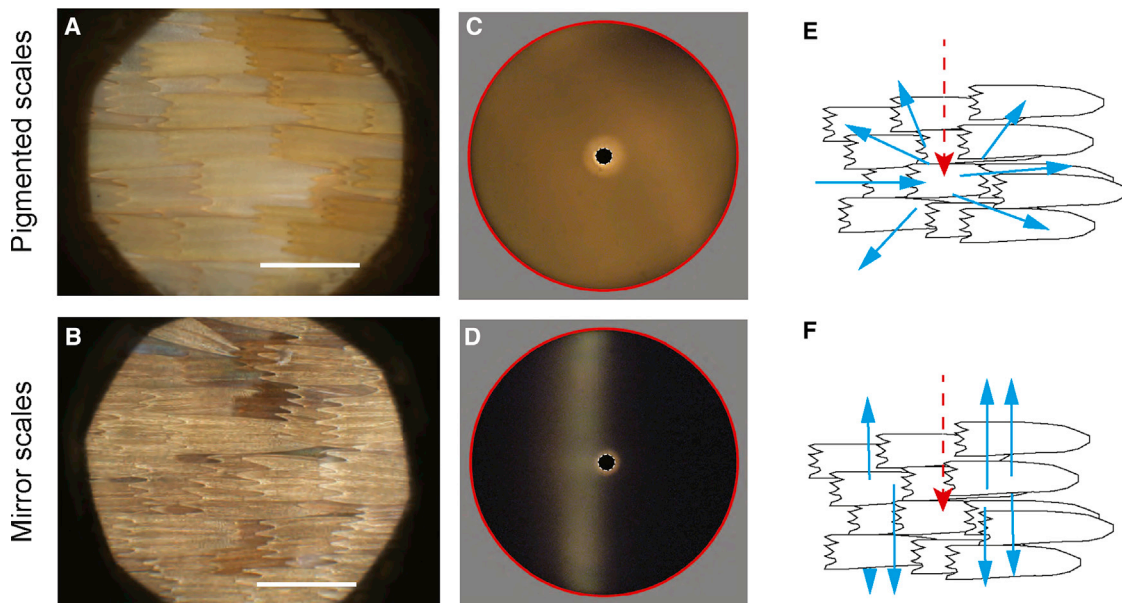


Figure 2. Spatial Reflectance Properties of “Mirror” Scales and Pigmented Scales from the Forewings

(A) Images of a small section of scale lattice (scale bar, 500 μm) on the wing reveal multidirectional scattering by the pigmented scales on the male's hindwing and (B) angle-dependent diffraction by the mirror scales on the male's forewing (see also Figure S3).

(C and D) The scatterograms of the isolated wing scales show that the pigmented scales generate a diffuse scattering pattern, while the mirror scales (D) scatter light highly directionally. The red circle in (C) and (D) corresponds to a scattering angle of $\sim 72^\circ$; the central area has been removed as it contains direct scattering from lens elements in the microscopy setup.

(E and F) The schematic shows the orientation of the scale lattice with respect to the body: pigmented scales scatter light in all directions (E), while the mirror scales scatter light perpendicular to the scale ridges (F).

the upper and lower laminae of the scales (Figure 3E [8]). There was no difference in the structure of the pigmented scales between the sexes. The bronze or “mirror” scales that are distributed throughout the surface of the female forewing, and that are solely present in the three discrete patches of the male forewing, differ drastically from this basic layout. In these scales, the spaces between the ridges and cross-ribs form partially closed windows, generating an almost continuous upper lamina (Figures 3C and 3D). We can understand the mirror effect by assuming that thin-film interference is generated both by the upper and by the lower lamina. Because the upper lamina is irregular, there is additive color mixing that produces a sparkly bronze effect (Figures 3F and 3G). While the pigmented scales are similarly structured in both males and females, this is not the case for the mirror scales. In males, the upper lamina of the mirror scales is consistently more closed (Figure 3H) than in females (Figure 3I), causing strong thin-film interference and explaining why the males' wing patches apparently disappear when the wings are normal with respect to incident light. As the upper lamina of females is largely open, thin-film interference is minimal and the upper lamina acts more like a diffuser, similar to the pigmented scales, resulting in the limited directionality in female patterning.

The dynamic changes in wing patterning in males are not explained by structural interference alone but also by stacking of the different scale types. The mirror scales are angled with respect to the wing surface and stacked above layers of pigmented scales (Figure 4). When incident light is near normal, the overlying mirror scales produce interference that results in additive color mixing and the observed sparkly bronze

appearance (Figure 4A). When the wing is tilted with respect to incident light, light scattered by the mirror scales is reflected outside the viewing direction and therefore not visible. The appearance of the dark patches in the males' wings is thus due to the combined absence of visible interference effects and the diffuse reflectance of the underlying melanin-pigmented scales (Figure 4B).

The successive appearance and disappearance of the males' three patches can be explained if the mirror scales lie at slightly different angles relative to the wing surface, so that the patches switch from observable interference effects to pigmentary coloration depending on tilt angle. We evaluated the tilt angle of the scales relative to the wing surface by performing reflectance goniometry on a wing patch in the mid forewing of a male. The polar reflectance plot (Figure 4C) for the mirror scales in patch 1 reveals maximal reflectance at $\sim 22^\circ$ for an angle of incidence of -30° . Using mirror geometry, the difference between the angle of incidence and the angle of peak reflectance (30° versus 22°) implies a scale tilt angle of $\sim 4^\circ$ ($2\theta = 8^\circ$, where θ is the angle of the mirror, i.e., scale). Our finding that scales outside these patches did not produce directional reflectance (Figure 4C) confirms that these special visual effects are produced by stacking of the specialized mirror scales and that the angle of scale stacking varies with the location of the scales on the male's wing.

Here, we describe a novel use of structural coloration that combines thin-film interference, stacking of the different scale types, and differential angling of the scales on the wing surface, to produce dynamic, achromatic wing patterning in a nocturnal

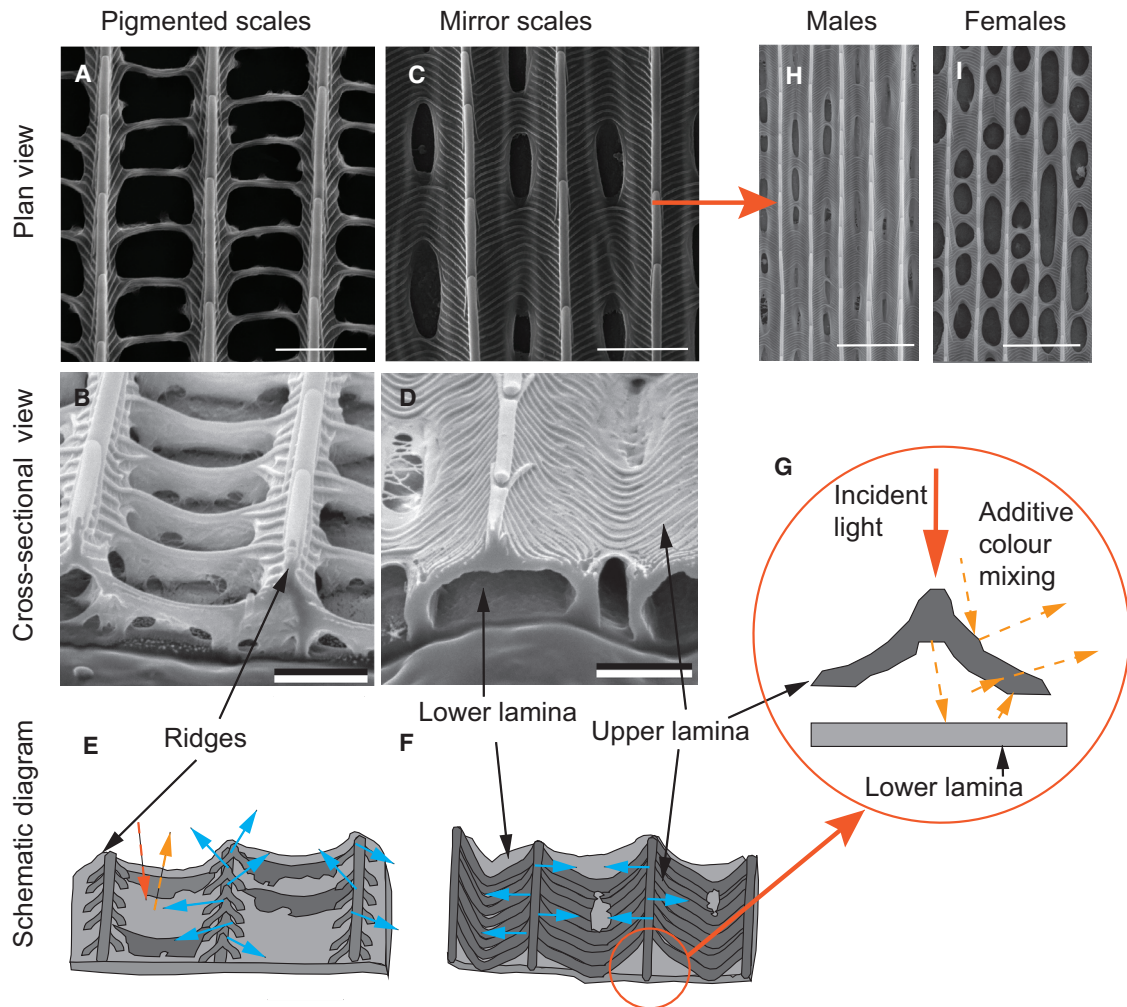


Figure 3. Ultrastructure of the “Mirror” Scales and the Pigmented Scales

(A and B) SEM images of the pigmented scales of a male in (A) plan view and in (B) oblique and cross-sectional view. In the pigmented scale, the cross ribs and ridges form an open lattice unstructured upper lamina so that the lower lamina is visible (scale bars, 20 μm).

(C and D) SEM images of the mirror scales of a male in (C) plan view and in (D) oblique and cross-sectional view. In the mirror scales, the spaces between the ridges (“windows”) are mostly closed, forming a continuous upper lamina that is present above the lower lamina (scale bars, 20 μm).

(E) A cross-sectional schematic of the pigmented scale structure shows multidirectional scattering off the scale ridges (blue arrows) and reflectance of light off the lower lamina (orange arrows).

(F) In the mirror scales, light is reflected in a direction perpendicular to the scale ridges (blue arrows).

(G) A schematic cross-sectional view shows that both the upper and lower lamina generate thin-film interference. The irregularity in the distance and thickness of each layer results in additive color mixing and an angle-dependent sparkly effect.

(H and I) The mirror scales differ in structure between the sexes; the upper lamina is more closed in (H) males than (I) females (scale bars, 5 μm).

moth. Structural coloration is well known for generating spectacular optical displays, such as the shimmering red/pink gorgets of hummingbirds [10] and the metallic luster of beetle wing cases [11] but is not known to produce directional patterning by superposing black patches created using melanin (black/brown). The scale nanostructures of male *E. materna* generate an angle-dependent shift in the area of patterning, rather than the switching on and off of hue and/or brightness, typical of structural coloration [12]. The combination of these effects is a dynamic optical signal with restricted angular visibility.

Structural coloration with broad angular reflectance, such as the iridescent blue wings of *Morpho* butterflies, is thought to

serve for long-range visual communication during flight [13]. Structural colors with limited angular reflectance, such as those on the ventral surface of swordtail butterflies (*Ancyluris meliboeus*), are, however, considered to optimize signal visibility when the animal is at rest [14]. Structural colors that are male limited and have restricted angular visibility can arise from female preferences for exaggerated male traits; in the eggfly butterfly (*Hypolimnas bolina*), for example, females prefer males with the brightest UV wing patches [15], but these patches are only visible over a narrow angular range ($\sim 20^\circ$) when the female views the male directly from above [16, 17]. Structural, male-limited coloration has the advantage of allowing the male to

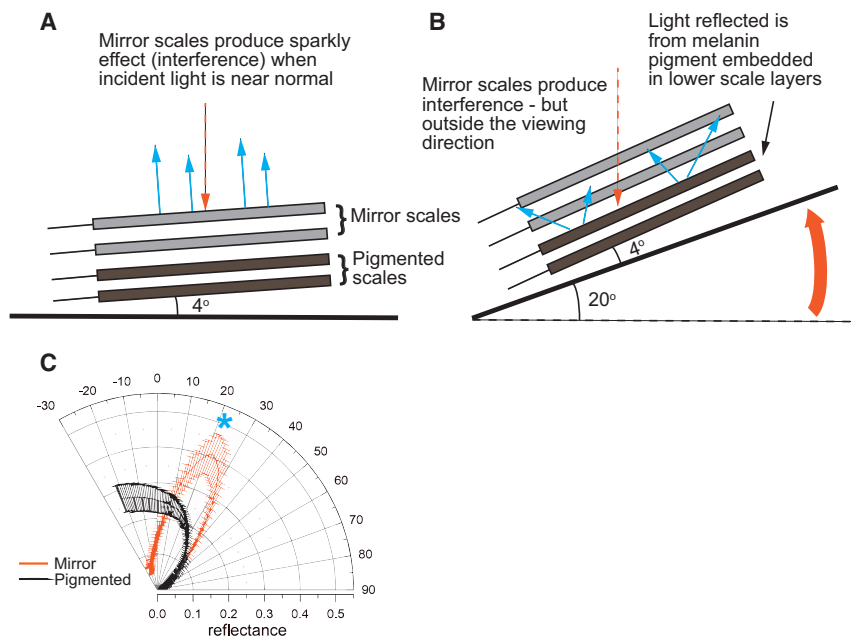


Figure 4. Dynamic Wing Patterning: A Combination of Thin-Film Interference and Scale Stacking

(A) The scales are stacked on the wing surface, with the pigmented scales underlying the mirror scales. Interference effects are generated by the mirror scales when incident light is about near normal.

(B) When the wing is rotated $\sim 20^\circ$ about the horizontal axis (roll), light interacting with the mirror scales is directionally reflected outside the viewing direction, resulting in the visibility of the diffuse scattering from the underlying melanin scales and the appearance of the black patches (see also Figure S4).

(C) Polar reflectance plot of the mirror scales (red) and the pigmented scales (black) for a fixed light incidence at -30° and scattering angle from -30° to 90° . The pigmented scales show a diffuse reflectance over a broad angular range, while the mirror scales show reflectance over a narrow angular range, peaking at $\sim 22^\circ$ (blue asterisk).

control the timing, direction, and strength of the signal by modifying his signaling behavior [18–20]. For example, male *H. bolina* orientate in a manner that maximizes the conspicuousness of the UV-iridescent patches during courtship [17].

Unfortunately, the reproductive behavior of the *Eudocima* genus investigated here remains largely unknown. Males tend to be more abundant in the early evening, with mating thought to occur from around midnight [6]. The limited angular visibility of the males' wing patches allows us to predict that the structure-induced black patch effect can be maximized for a given viewing direction, when changes in patterning primarily result from variation in male orientation with respect to the viewer. If the male rests on a vertical surface with its wings opened, the dark wing patches would not be visible to an observer perpendicular to the wing surface but would only show up strongly at angles $\sim 20^\circ$ – 30° away from the vertical (Figure S4). The optical effect is particularly prominent if a female views a male from above and to the side, as in most other Lepidoptera [17]. Male noctuids often vigorously vibrate the wings in pre-flight before approaching the female [21], resulting in the wing patches rapidly flashing on and off depending on the wingbeat frequency. Flash stimuli are known to evoke a super-normal visual response in butterflies [5] and could function to increase the conspicuousness and attractiveness of the visual signal [17]. The dynamic stimulus would be particularly effective under directional lighting, which is more likely in the arid habitats that are preferred by *E. materna* [6], although we note that the angle-dependent effects also operate under diffuse lighting conditions.

Our indirect evidence that the wing patterns of a nocturnal moth might function as a visual signal is highly unusual because nocturnal Lepidopterans are considered to rely almost exclusively on pheromones for sexual communication [22]. Female moths “call” by releasing a sex attractant, and many species of male noctuid respond by flying upwind to the female and releasing pheromones from their abdominal brush organ [21].

However, there is some evidence that once the male has located a female, visual and tactile cues may play a role in mediating courtship. For example, male codling moths (*Laspeyresia pomonella*) spend more time walking, wing fanning, and attempting to copulate when multiple cues are present than olfactory cues alone [23]. The use of visual cues in courtship appears to be more common in day-flying moths, with males (e.g., *Paysandisia archon*; family Castniidae) using visual cues to patrol territories and to locate and chase females [24]. The courtship behavior of nocturnal Lepidoptera is not well known [21], particularly with respect to selection on wing coloration [25], and detailed studies of the role of vision are required to understand visual signaling in dim light.

Nocturnal illumination is orders of magnitude lower than daylight, yet many nocturnal animals, including moths, have remarkable visual adaptations that allow them to perform essential behaviors such as orientation, navigation, and foraging at night [26]. For example, nocturnal hawkmoths use spatial and temporal summation to increase contrast sensitivity in low light, but at the cost of spatial and temporal resolution [27]. A few nocturnal animals, including hawkmoths, have color vision, which is used to guide foraging decisions at night [28, 29]. Diurnal hawkmoths are also sensitive to the visual information provided by patterning and show a preference for radial patterns that are representative of foraging targets [30, 31]. Our intriguing findings on the dynamic wing patterning of the male Dot-underwing moth will inspire novel research directions on nanostructure optics, visual processing in dim light, and the evolution and function of nocturnal visual signals.

STAR★METHODS

Detailed methods are provided in the online version of this paper and include the following:

- KEY RESOURCES TABLE
- LEAD CONTACT AND MATERIALS AVAILABILITY

- **EXPERIMENTAL MODEL AND SUBJECT DETAILS**
 - Moth subjects
- **METHOD DETAILS**
 - Angle-dependent wing pattern evaluation
 - Wing image analysis
 - Spectrophotometry and k-space imaging
 - Scanning Electron Microscopy (SEM)
- **QUANTIFICATION AND STATISTICAL ANALYSIS**
 - Modeling change in patch size with wing angle in males
- **DATA AND CODE AVAILABILITY**

SUPPLEMENTAL INFORMATION

Supplemental Information can be found online at <https://doi.org/10.1016/j.cub.2019.07.005>.

ACKNOWLEDGMENTS

We thank Jan Hemmi for use of the goniometer, Cédric Kilchoer for technical support, and Stefano De Faveri for information and access to video footage. We thank Thomas White and Doekele Stavenga for comments on the manuscript and Andy Young, Crystal Klem, and Alberto Zilli for information on the *Eudocima* moths. We are grateful for the constructive comments of two anonymous reviewers that improved our work. This study was supported by the Swiss National Science Foundation through Ambizione programme grant 168223 (to B.D.W.) and the National Center of Competence in Research Bio-Inspired Materials (to B.D.W.). J.L.K. was funded by an Australian Research Council (ARC) Future Fellowship (FT180100491).

AUTHOR CONTRIBUTIONS

Conceptualization, J.L.K., J.A.E., and B.D.W.; Investigation, N.J.T., G.E.S.-T., J.L.K., and B.D.W.; Writing – Original Draft, J.L.K. and B.D.W.; Visualization, B.D.W. and J.L.K.; Writing – Review & Editing, J.L.K., N.J.T., G.E.S.-T., J.A.E., and B.D.W.

DECLARATION OF INTERESTS

The authors declare no competing interests.

Received: April 3, 2019

Revised: May 28, 2019

Accepted: July 1, 2019

Published: August 8, 2019

REFERENCES

1. Brakefield, P.M., and French, V. (1999). Butterfly wings: the evolution of development of colour patterns. *BioEssays* 21, 391–401.
2. Sekimura, T., and Nijhout, H.F. (2017). Diversity and Evolution of Butterfly Wing Patterns (Springer Nature).
3. Nijhout, H.F. (1981). The color patterns of butterflies and moths. *Sci. Am.* 245, 140–153.
4. Doucet, S.M., and Meadows, M.G. (2009). Iridescence: a functional perspective. *J. R. Soc. Interface* 6 (Suppl 2), S115–S132.
5. Magnus, D.B.E. (1957). Experimental analysis of some 'overoptimal' sign stimuli in the mating behaviour of the fritillary butterfly, *Argynnis paphia*. *Proc. Int. Congr. Entomol.* 2, 405–418.
6. Fay, H., and Halfpapp, K. (1999). Activity of fruit-piercing moths, *Eudocima* spp. (Lepidoptera: Noctuidae), in north Queensland crops: Some effects of fruit type, locality and season. *Aust. J. Entomol.* 38, 16–22.
7. Vignolini, S., Moyroud, E., Glover, B.J., and Steiner, U. (2013). Analysing photonic structures in plants. *J. R. Soc. Interface* 10, 20130394.
8. Stavenga, D.G., Leertouwer, H.L., and Wilts, B.D. (2014). Coloration principles of nymphaline butterflies - thin films, melanin, ommochromes and wing scale stacking. *J. Exp. Biol.* 277, 2171–2180.
9. Nijhout, H. (1997). Ommochrome pigmentation of the linea and rosa seasonal forms of *Precis coenia* (Lepidoptera: Nymphalidae). *Arch. Insect Biochem. Physiol.* 36, 215–222.
10. Giraldo, M.A., Parra, J.L., and Stavenga, D.G. (2018). Iridescent colouration of male Anna's hummingbird (*Calypte anna*) caused by multilayered barbules. *J. Comp. Physiol. A Neuroethol. Sens. Neural Behav. Physiol.* 204, 965–975.
11. Seago, A.E., Brady, P., Vigneron, J.-P., and Schultz, T.D. (2009). Gold bugs and beyond: a review of iridescence and structural colour mechanisms in beetles (Coleoptera). *J. R. Soc. Interface* 6 (Suppl 2), S165–S184.
12. Silberglied, R.E. (1984). Visual communication and sexual selection among butterflies. In *The Biology of Butterflies*, R.I. Vane-Wright, and P.R. Ackery, eds. (Academic Press), pp. 207–223.
13. Vukusic, P., Sambles, J.R., Lawrence, C.R., and Wootton, R.J. (1999). Quantified interference and diffraction in single *Morpho* butterfly scales. *Proc. Biol. Sci. B.* 266, 1403–1411.
14. Vukusic, P., Sambles, J.R., Lawrence, C.R., and Wootton, R.J. (2002). Limited-view iridescence in the butterfly *Ancyluris meliboeus*. *Proc. Biol. Sci.* 269, 7–14.
15. Kemp, D.J. (2007). Female butterflies prefer males bearing bright iridescent ornamentation. *Proc. Biol. Sci.* 274, 1043–1047.
16. Kemp, D.J., and Macedonia, J.M. (2006). Structural ultraviolet ornamentation in the butterfly *Hypolimnas bolina* L. (Nymphalidae): visual, morphological and ecological properties. *Aust. J. Zool.* 54, 235–244.
17. White, T.E., Zeil, J., and Kemp, D.J. (2015). Signal design and courtship presentation coincide for highly biased delivery of an iridescent butterfly mating signal. *Evolution* 69, 14–25.
18. Poulton, E.B. (1890). *The Colours of Animals, Their Meaning and Use, Especially Considered in the Case of Insects* Volume 67 (D. Appleton and Company).
19. Hamilton, W.J., III. (1965). Sun-oriented display of the Anna's hummingbird. *Wilson Bull.* 77, 38–44.
20. Endler, J.A. (1983). Natural and sexual selection on color patterns in Poeciliid fishes. *Environ. Biol. Fishes* 9, 173–190.
21. Birch, M. (1970). Pre-courtship use of abdominal brushes by the nocturnal moth, *Phlogophora meticulosa* (L.) (Lepidoptera: Noctuidae). *Anim. Behav.* 18, 310–316.
22. Hansson, B.S. (1995). Olfaction in Lepidoptera. *Experientia* 51, 1003–1027.
23. Castrovillo, P.J., and Carde, R.T. (1980). Male codling moth (*Laspeyresia pomonella*) orientation to visual cues in the presence of pheromone and sequences of courtship behaviors. *Ann. Entomol. Soc. Am.* 73, 100–105.
24. Sarto i Monteys, V., Acín, P., Rosell, G., Quero, C., Jiménez, M.A., and Guerrero, A. (2012). Moths behaving like butterflies. Evolutionary loss of long range attractant pheromones in castniid moths: a *Paysandisia archon* model. *PLoS ONE* 7, e29282.
25. Allen, C.E., Zwaan, B.J., and Brakefield, P.M. (2011). Evolution of sexual dimorphism in the Lepidoptera. *Annu. Rev. Entomol.* 56, 445–464.
26. Warrant, E.J. (2017). The remarkable visual capacities of nocturnal insects: vision at the limits with small eyes and tiny brains. *Philos. Trans. R. Soc. Lond. B Biol. Sci.* 372, 20160063.
27. Stöckl, A.L., O'Carroll, D.C., and Warrant, E.J. (2016). Neural summation in the hawkmoth visual system extends the limits of vision in dim light. *Curr. Biol.* 26, 821–826.
28. Kelber, A., Balkenius, A., and Warrant, E.J. (2002). Scotopic colour vision in nocturnal hawkmoths. *Nature* 419, 922–925.

29. Somanathan, H., Borges, R.M., Warrant, E.J., and Kelber, A. (2008). Nocturnal bees learn landmark colours in starlight. *Curr. Biol.* **18**, R996–R997.
30. Kelber, A. (1997). Innate preferences for flower features in the hawkmoth *Macroglossum stellatarum*. *J. Exp. Biol.* **200**, 827–836.
31. Kelber, A. (2002). Pattern discrimination in a hawkmoth: innate preferences, learning performance and ecology. *Proc. Biol. Sci.* **269**, 2573–2577.
32. R Development Core Team (2016). R: A Language and Environment for Statistical Computing, 3.3.3 Edition (R Foundation for Statistical Computing).
33. Schneider, C.A., Rasband, W.S., and Eliceiri, K.W. (2012). NIH Image to ImageJ: 25 years of image analysis. *Nat. Methods* **9**, 671–675.
34. Troscianko, J., and Stevens, M. (2015). Image calibration and analysis toolbox - a free software suite for objectively measuring reflectance, colour and pattern. *Methods Ecol. Evol.* **6**, 1320–1331.

STAR★METHODS

KEY RESOURCES TABLE

REAGENT or RESOURCE	SOURCE	IDENTIFIER
Deposited Data		
Raw data	This paper	https://doi.org/10.17632/2r69bhwj59.1
Experimental Models: Organisms/Strains		
Dot Underwing moth, <i>Eudocima materna</i>	The Western Australian Museum, Perth, Australia.	N/A
Dot Underwing moth, <i>Eudocima materna</i>	The Bug Maniac	http://www.thebugmaniac.com/
Software and Algorithms		
Nikon View NX2 version 2.7.3	Nikon	N/A
R Software	[32]	R Project for Statistical Computing; RRID: SCR_001905
ImageJ software	[33]	ImageJ; RRID: SCR_003070
Mica Toolbox for ImageJ	[34]	http://www.empiricalimaging.com/
Other		
Universal Stage goniometer	Leitz, Wetzlar, Germany.	N/A
Nikon D7100 DSLR	Nikon, Tokyo, Japan	N/A
Maya LSL Spectrometer	Ocean Optics, Dunedin, FL, USA.	N/A
Zeiss Axio Scope A1 light microscope	Zeiss, Oberkochen, Germany	N/A
Point Gray Grasshopper 3 camera	FLIR, Richmond, Canada.	N/A
Tescan Mira 3 field-emission scanning electron microscope	Tescan, Kohoutovice, Czech Republic.	N/A
FEI Scios 2 dual-beam focused ion-beam scanning electron microscope	Thermo Fisher Scientific, Waltham, MA, United States	N/A

LEAD CONTACT AND MATERIALS AVAILABILITY

Further information and requests for resources and reagents should be directed to and will be fulfilled by the Lead Contact, Jennifer Kelley (jennifer.kelley@uwa.edu.au). This study did not generate new unique reagents.

EXPERIMENTAL MODEL AND SUBJECT DETAILS

Moth subjects

Mounted specimens of *E. materna*, collected from the Kimberley (Koolen Island and Cockatoo Island) and Pilbara (Millstream-Chichester National Park) regions of northwest Western Australia, were obtained from the Western Australian Museum in Perth, Australia. A total of five museum specimens were used for the wing pattern evaluation, three males and two females (forewing lengths males: 1 = 42.7, 2 = 40.7, 3 = 42.3mm; females: 1 = 44.2, 2 = 42.9mm). An additional two mounted specimens (one of each sex) were obtained from a commercial supplier (thebugmaniac.com) to investigate the nanostructure of the wing scales.

METHOD DETAILS

Angle-dependent wing pattern evaluation

To investigate angle-dependent wing patterning, we used a Universal Stage goniometer (Leitz, Wetzlar, Germany) to rotate moths along the long or horizontal axis (roll), and perpendicular to the long body axis (pitch), while keeping the illumination source fixed and overhead. Moths were mounted on the stage of the goniometer and photographed with a Nikon D7100 DSLR fitted with 60mm Nikon macro lens and a Meike FC100 LED macro ring flash which illuminated over a total solid angle of 80°. A scale bar was included in each image for subsequent measurement of wing sizes. The left and right wings were photographed separately for rotation toward and away from the direction of incident light (i.e., 40° in each direction), where 0° is the wing position perpendicular to the camera (n = 162 images/individual for roll). This process was repeated for wing pitch, but over five-degree increments (n = 34 images/individual for pitch), since changes in patch size were less apparent with rotation about the vertical axis.

Wing image analysis

Wing images were captured in RAW format and converted to .TIF (16-bit) files without compression using Nikon View NX2 software version 2.7.3 (Nikon Corporation, Tokyo). We used the wand tool in the image analysis program ImageJ [33] (<https://imagej.nih.gov/ij/>) to trace and measure the area of each of the males' three wing patches, which we designated as patches 1-3, moving in the direction closest to the body (i.e., patch 1) and toward the wing tips (i.e., patch 3) (Figure 1). The wand was used to select automatically a contiguous area of similar pixel values within a tolerance range of 2000. Preliminary trials with different tolerance ranges revealed that this value allowed for optimal selection of the males' patches. The area of each selected patch, and the total area of patches, was then measured (in mm²) with reference to the measurement calibration grid scale included in each image. Although the wing patches change in apparent size as the wing is rotated irrespective of any changes in directional reflectance (because patches that are further away would appear smaller), we chose not to correct for this, as this is how the patches would be viewed by predators or conspecifics. Specifically, it is the area of the patch that is subtended on the viewer's eye that is important – not absolute patch size. All images were thus adjusted to size using the scale bar photographed at a wing angle of 0° to the camera lens. We used these same imaging methods to measure the maximum patch size in males and females for both the left and the right forewings.

Females tended to display subtle wing darkening with changing angle, rather than changes in patch size. The female angle-dependent patterning was quantified by focusing on changes in wing reflectance with movement toward and away from the light (a range of 40° in each direction) using increments of 5°. RAW images were linearized using the image calibration and analysis tool Mica Toolbox [34] for ImageJ, using a customized greyscale standard of known reflectance. Subsequently, the green channel of each calibrated image was used to calculate the mean percentage reflectance (averaged over the total area of bronze/brown coloration) of each wing at each angle to the incident light. The green channel is in the mid-range of the spectrum and preliminary investigations revealed that this channel produced the most pattern information.

Spectrophotometry and k-space imaging

Reflectance spectra from different areas of the wings were obtained using a bifurcated probe connected to a halogen-deuterium light source and an Ocean Optics Maya LSL (Ocean Optics, Dunedin, FL, USA) diode-array spectrometer. The probe was positioned normal to the wing surface and measurements were made with reference to a diffuse white reflection standard (WS-1, Ocean Optics). Reflectance spectra of single scales were measured in a custom-adapted Zeiss Axio Scope A1 light microscope (Zeiss, Oberkochen, Germany). Light reflected from the sample was focused on a confocally-placed optical fiber via a mirror and analyzed using the Ocean Optics Maya LSL spectrometer. *K*-space imaging uses conoscopic imaging and spectrometry to determine the directionality of the scattered beam, or the *k*-space distribution [7]. For *k*-space imaging of individual moth scales, a Bertrand lens (Zeiss) was inserted into the detection pathway and imaged using a Point Gray Grasshopper 3 camera (FLIR, Richmond, Canada).

Scanning Electron Microscopy (SEM)

The structure of isolated wing scales was investigated using a Tescan Mira 3 field-emission scanning electron microscope (SEM). Cross-sections were imaged using a FEI Scios 2 focused ion-beam-SEM and cut using a beam current of 0.3 nA at 30 kV using Ga ions. Scales were sputtered with a ~3 nm layer of platinum/ palladium (80: 20 wt%) prior to imaging to prevent charging.

QUANTIFICATION AND STATISTICAL ANALYSIS

Modeling change in patch size with wing angle in males

The wing angle with respect to the illumination source (in degrees) was plotted against patch area (in mm²) for each male and for each wing, where wing movements toward the light were considered positive angles and wing movements away from the light were considered negative angles. All figures display wing pattern data plotted separately for each individual. A polynomial function (where x = wing angle and y = patch size) was fitted to the resulting curves to examine the angle at which the patches were maximized for area, and also to determine whether this differed between the left and right wings and among individual males. We used the software program R [32] to examine the fit of different order polynomial functions to the data and to select the best model based on the R-squared values.

DATA AND CODE AVAILABILITY

The datasets generated during this study are available at <https://doi.org/10.17632/2r69bhwj59.1>.